

Intrinsic brain activity triggers trigeminal meningeal afferents in a migraine model

HAYRUNNISA BOLAY¹, UWE REUTER¹, ANDREW K. DUNN², ZHIHONG HUANG¹, DAVID A. BOAS²
& MICHAEL A. MOSKOWITZ¹

¹Stroke and Neurovascular Regulation Laboratory and ²NMR Center, Department of Radiology, Massachusetts General Hospital, Harvard Medical School, Boston, Massachusetts, USA

H.B., U.R. and A.K.D. contributed equally to this study.

Correspondence should be addressed to M.A.M.; email: moskowitz@helix.mgh.harvard.edu

Although the trigeminal nerve innervates the meninges and participates in the genesis of migraine headaches, triggering mechanisms remain controversial and poorly understood. Here we establish a link between migraine aura and headache by demonstrating that cortical spreading depression, implicated in migraine visual aura, activates trigeminovascular afferents and evokes a series of cortical meningeal and brainstem events consistent with the development of headache. Cortical spreading depression caused long-lasting blood-flow enhancement selectively within the middle meningeal artery dependent upon trigeminal and parasympathetic activation, and plasma protein leakage within the dura mater in part by a neurokinin-1-receptor mechanism. Our findings provide a neural mechanism by which extracerebral cephalic blood flow couples to brain events; this mechanism explains vasodilation during headache and links intense neurometabolic brain activity with the transmission of headache pain by the trigeminal nerve.

Although approximately 15–20% of the general population suffers from migraine headaches, little is known about its pathogenesis. The headaches are often associated with stress, emotion or sleep disturbance, but the role of brain in migraine is still controversial. The brain is traditionally viewed as an insensate organ, but the meninges, comprising dura mater and leptomeninges (pia mater and arachnoid), are among the few pain-sensitive tissues within the cranium^{1–3}. The meninges are densely innervated by small-caliber trigeminal axons⁴, some of which bifurcate⁵ in proximity to small blood vessels branching from the middle cerebral (pial) and middle meningeal (dural) arteries^{6–8}. Despite species differences in brain size and organizational complexity, trigeminal innervation appears remarkably similar in mammals such as the rat⁹, cat⁴ and human¹⁰, and it contains the same constellation of peptide neurotransmitters. When stimulated experimentally in humans, large vessels in the dura and pia mater generate throbbing unilateral migraine-like pain², and hence the term trigeminovascular system was coined.

One form of migraine is preceded by visual aura that starts 20–40 minutes before and is characterized by spreading scintillations reflecting a slow propagation of neuronal and glial excitation emanating from one occipital lobe. Recent blood oxygenation level-dependent (BOLD) functional magnetic resonance imaging^{11,12} and positron emission tomography¹³ studies confirm the original suggestion made by Leao¹⁴ that cortical spreading depression (CSD) within the occipital lobe generates the visual aura experienced by 20% of migraineurs. CSD is characterized by dramatic shifts in cortical steady potential (DC), significant transient increases in extracellular ions and neurotransmitters such as glutamate, and transient increases in cortical blood flow followed by sustained flow decreases. After the aura, headaches develop especially on the side of the af-

ected hemisphere. Although a link between aura and headache was suspected¹⁵, the cause for the pain remains unknown. Because the trigeminal nerve transmits cephalic pain and each trigeminal nerve projects primarily to one side, we therefore tested whether intense perturbations in cortical neuro-metabolic activity such as in cortical spreading depression provoke or discharge trigeminal axons innervating the meninges.

CSD induces long-lasting blood-flow increase in MMA

Using the novel technique of laser speckle-contrast imaging¹⁶, we obtained two-dimensional maps of blood flow within cerebral cortex, pial vessels and middle meningeal artery (MMA) (Fig. 1a) with high spatio-temporal resolution (Fig. 1). Speckle contrast images (Fig. 1a) at different time-points were used to generate relative blood-flow maps (Fig. 1b–d). Immediately after pricking the cortical surface with a pin 7–9 mm away from the MMA, relative blood flow did not change in the imaged area (Fig. 1b). Approximately three minutes later, a large transient (lasting < 2 min) increase in blood flow was observed in cortex ($250 \pm 20\%$ of baseline; $n = 9$) and in pial vessels ($205 \pm 20\%$ of baseline, not different from cortical flow values, $P > 0.05$). These changes propagated across the cortical surface in one hemisphere contemporaneous with neuronal and glial depolarization. At this early time-point, transient (< 2 min) blood-flow increases ($127 \pm 4\%$ of baseline, $n = 9$) were detected within the MMA as the cortical hyperemia spread beneath the MMA (P1) (Fig. 1c).

The most striking and sustained blood-flow increase occurred selectively within the MMA (P2) and accompanying vein, beginning approximately five minutes after evoking CSD (Fig. 1d and e). Reaching a peak of $137 \pm 5\%$ above baseline at around 15 minutes, the MMA blood flow remained elevated for

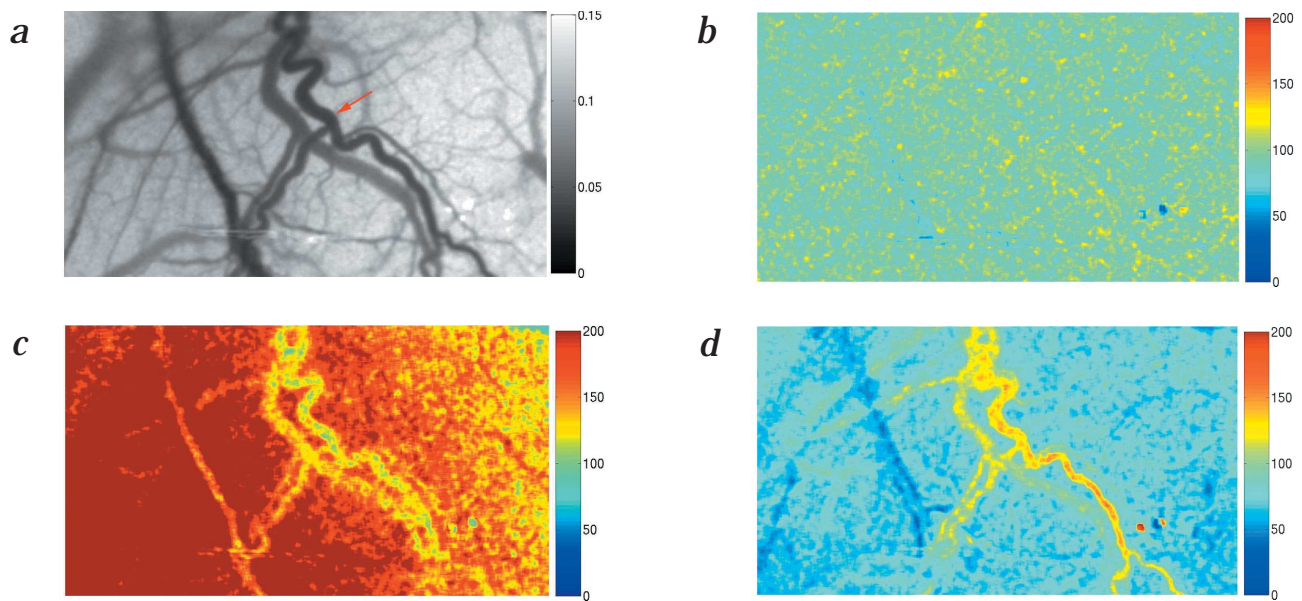


Fig. 1 Blood-flow images of MMA following CSD. Laser-speckle images of blood flow in MMA and underlying parietal cortex and pial vessels following a single CSD. CSD was induced 7–9 mm anterior (left) to the area imaged (1.75×2.5 mm). **a**, Speckle contrast image demonstrating the spatial flow heterogeneities across the imaged area at a single time illustrating MMA (arrow; proximal vessel is at top) and associated dural vein plus pial vessels and cerebral cortex. The darker values correspond to higher blood flow. **b–d**, Relative blood-flow maps expressed as percentage of baseline, during the temporal evolution of CSD and represented by pseudo-colored images at the time-points shown in **e**. **b**, Imaged blood flow after CSD induction, but prior to propagation of cortical hyperemia into the imaged area showing no immediate changes. **c**, Cortical hyperemia (dark red) spreading from anterior to posterior (left to right) during CSD. Note that the marked flow increase in cortex and overlying pial vessels was comparable during CSD. A smaller transient rise in MMA blood flow (125% of baseline) was detected at this time. **d**, Blood-flow map taken 20 min after CSD induction showing selective elevation of flow in MMA (140% of baseline) as well as in a dural vein. The relative blood flow in pial vessels and cortex is below baseline at this time (80% of baseline).

e, The time-course of the change in relative blood flow in MMA (red line) and cerebral cortex (blue line) demonstrates that CSD induces biphasic blood-flow elevations within MMA with an early transient peak (P1) coincident with cortical hyperemia. A slower and more sustained increase in MMA blood flow (P2) is observed for approximately 45 min; **b**, **c**, and **d** denote the time points of corresponding images in **b**, **c**, **d**.

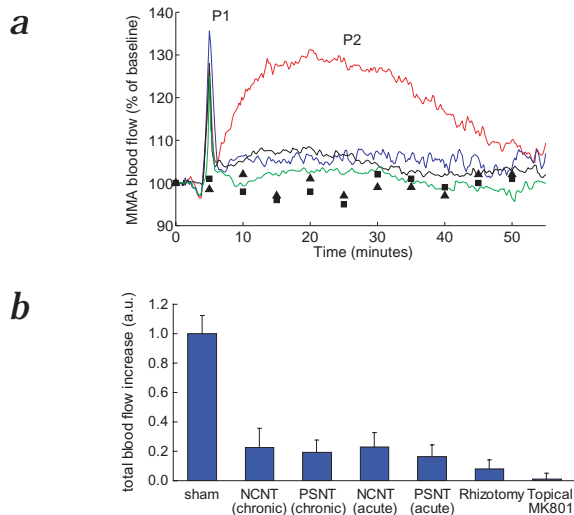
an additional 10 minutes, and returned to baseline within 45 minutes (Fig. 1d). During this time, a slight decrease ($90 \pm 3\%$ of baseline) was observed in cortical blood flow (oligemia) as well as in pial vessels (Fig. 1d). Flow changes were strictly confined to the side of the affected hemisphere and overlying meninges and did not appear when CSD was evoked in the contralateral hemisphere ($n = 4$) (Fig. 2a). To evaluate the importance of traumatic injury (pinprick) to MMA blood flow, topical MK-801, which is a N-methyl-D-aspartate receptor antagonist, was applied to the cortical pinprick site. MK-801 blocked CSD propagation as well as the neurovascular response in MMA ($n = 5$) (Fig. 2a and b) thereby suggesting that CSD and not trauma caused MMA blood-flow augmentation.

Because the speckle-contrast imaging technique acquires information from the upper $500 \mu\text{m}$ of cortex and dura¹⁶, it is possible that the values for the MMA blood-flow measurements were slightly affected by the underlying cortical blood flow beneath the MMA. Therefore, the values for the MMA blood flow during the early peak (P1) could be partly due to the underlying cortical blood-flow increase, and therefore the actual MMA blood flow may be overestimated at this time-point. In con-

trast, the values for the sustained blood-flow increase in the MMA (P2) may be slightly underestimated, as the cortical tissue beneath the MMA is oligemic whereas the MMA blood flow is elevated. We therefore measured changes in vessel diameter to confirm the blood-flow changes using an independent method in selected experiments. Accompanying the blood-flow changes noted above, we detected a MMA vasodilation ($\sim 10\%$ diameter change, $n = 4$) during P1 and P2 suggesting that the MMA blood-flow changes (especially during P1) were not significantly affected by underlying cortical blood flow in this experiment.

Thus, under the stated experimental conditions, cortical events not only transiently increase local blood flow within brain, but also augment and prolong flow and dilation in extracerebral cephalic blood vessels such as the MMA.

To determine whether the MMA blood-flow response was dependent upon trigeminal innervation, we repeated the above experiments after chronic (10–14 d) unilateral transection of the trigeminal branch innervating the meninges (nasociliary nerve or NCN). By so doing, the delayed (P2), but not acute (P1), rise in MMA blood flow was abrogated (Fig. 2). The P1 rise



in the intact versus denervated animals was $127 \pm 4\%$ ($n = 9$) and $134 \pm 3\%$ ($n = 7$), respectively ($P > 0.05$), and was therefore not caused by trigeminal activation. The P2 peak elevation decreased markedly from $137 \pm 5\%$ ($n = 9$) to $105 \pm 2\%$ ($n = 7$), respectively on the intact and denervated side ($P < 0.001$), whereas the integrated blood-flow response during P2 decreased by 75% (Fig. 2b). Because trigeminal stimulation initiates a reflex-like increase in cortical blood flow by stimulating parasympathetic efferents¹⁷, we next examined whether the dural blood-flow response decreased after sectioning postganglionic parasympathetic fibers projecting from the sphenopalatine ganglia. Again, the P1 response was not significantly changed ($P > 0.05$) (Fig. 2); however, the delayed increase in flow (P2) was abrogated in intact and denervated sides ($n = 11$, $P < 0.001$) (Fig. 2), and the integrated blood-flow response was reduced by 80% (Fig. 2b). Acute transection of NCN ($n = 9$) or parasympathetic efferents ($n = 7$) gave the same results (Fig. 2b). After sectioning the trigeminal root, P2 was reduced like after nerve transection ($n = 6$) (Fig. 2b). These data indicate that

Fig. 2 Sustained blood-flow response in MMA is neurogenically mediated. **a**, Relative MMA blood flow during CSD after sham operation (red line) or chronic sectioning of the trigeminal (nasociliary nerve; NCNT, blue line) or parasympathetic (PSNT, black line) nerves supplying the meninges, or the trigeminal root (rhizotomy, green line). Chronic NCNT or PSNT significantly reduced the prolonged MMA blood-flow rise (P2) following CSD. In normal animals, the mean P2 increase reached $137 \pm 5\%$ of baseline, but it was abolished after NCN transection ($105 \pm 2\%$), PSN transection ($107 \pm 2\%$) or trigeminal rhizotomy ($103 \pm 2\%$, $P < 0.001$). Note that the early transient peak (P1) was unaffected by transection. Pinprick to the cortex itself did not change blood flow (■) when the CSD propagation was blocked by topical MK-801. CSD also did not change blood flow in contralateral dura mater (▲). **b**, Integrated blood-flow responses (P2; arbitrary units) following CSD in the following groups: control (sham-operated), chronic and acute trigeminal or parasympathetic transection, trigeminal rhizotomy and topical MK-801. Data are presented as mean \pm s.e.m.

the delayed and sustained blood-flow elevation (P2) was neurogenically mediated by parasympathetic efferents through brainstem connections, and was not due primarily to release of calcitonin gene-related peptide (CGRP) from trigeminal perivascular afferents, which are an important source of vasodilation and increased blood flow¹⁸.

A neurogenically mediated blood-flow rise was not observed in pial vessels or cortex, despite a dense trigeminal and parasympathetic innervation. Instead, oligemia was detected, probably because intrinsic blood-flow regulating mechanisms are suppressed during CSD as they are after migraine aura¹¹.

CSD causes plasma protein extravasation in dura mater

Trigeminal axons projecting to the meninges contain vasoactive neuropeptides (such as substance P, CGRP and neurokinin A) that promote plasma protein leakage and vasodilation within dura mater characteristic of neurogenic inflammation when released¹⁹. We reasoned that if CSD stimulates trigeminal axon collaterals innervating the leptomeninges, plasma proteins should leak from dural blood vessels that normally lack a blood-brain barrier. Horseradish peroxidase (HRP) was infused intravenously (i.v.) (60 mg/kg) to detect plasma protein extravasation. Like the blood-flow response, significant leakage occurred ($n = 12$) following even a single CSD ($n = 4$) (Fig. 3a and b). Edema was most prominent surrounding proximal middle meningeal blood vessels, and the intensity and distribution of edema was significantly higher on the ipsilateral side (CSD side/control side, 1.8 ± 0.1 ; $P < 0.001$, $n = 12$).

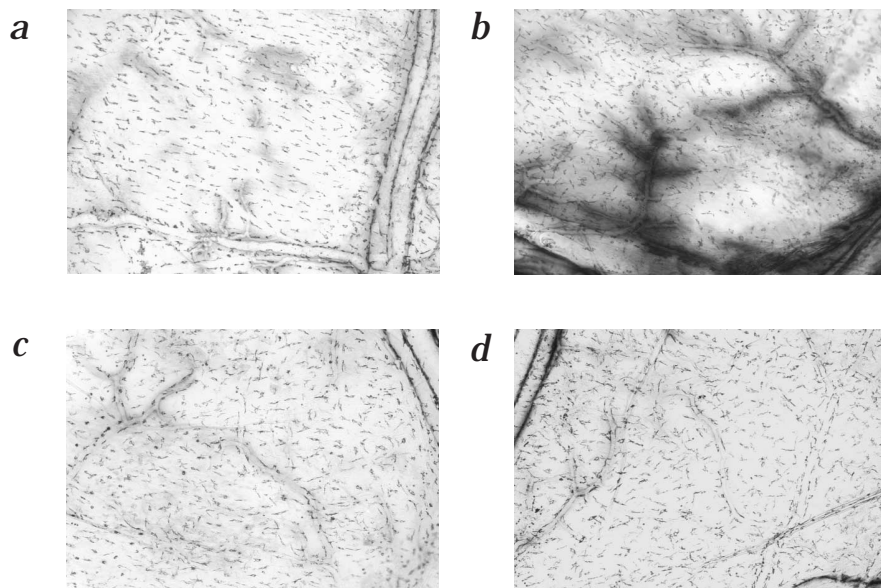


Fig. 3 Protein leakage in dura mater following CSD. **a-d**, Whole-mount preparations of dura mater showing leakage of horseradish peroxidase tracer from blood vessels following CSD in a normal rat ($\times 100$, light microscopy) (a and b) and in a rat after chronic trigeminal transection (c and d). a and b, As compared with the control side (a), significant perivascular leakage was detected surrounding meningeal vessels ipsilaterally after a single CSD (b) than on control side. NCNT blocked peroxidase extravasation (d) to levels approximating the control side (c).

To investigate the importance of neurogenic mechanisms in edema formation, we evaluated whether chronic NCN transection decreased protein extravasation. Ipsilateral trigeminal denervation blocked the CSD induced leakage (0.7 ± 0.1 , $n = 6$) and the difference between the two sides was not significant ($P > 0.05$) (Fig. 3c and d). To evaluate the effect of substance P on protein leakage, we blocked neurokinin-1 (NK1) receptors with L-733,060 (1 mg/kg, i.v.). Pretreatment suppressed edema formation (1.3 ± 0.3 , CSD side compared with the control side after L-733,060; $n = 6$), suggesting the importance of the NK1 receptor. By contrast to trigeminal nerve sectioning, chronic parasympathetic denervation did not decrease CSD-induced plasma protein leakage (2.1 ± 0.3 , comparing the CSD with control sides; $n = 5$).

CSD activates ipsilateral TNC

To test whether second-order neurons in trigeminal nucleus caudalis (TNC) are activated by CSD, we examined the expression of c-fos as a surrogate marker of neuronal activity²⁰. The number of c-fos-expressing cells is useful for mapping functionally related pathways and as a correlative indicator of TNC neuronal activity following noxious stimulation, despite the unclear relationship between nociceptor transmission and expression of this gene product. Fos was expressed on the side corresponding to the CSD predominantly in laminae I and II and mainly in ventral TNC, the termination site for the ophthalmic trigeminal division. The number of labeled cells was significantly higher especially in caudal TNC (Table 1), whereas differences were not significant in more rostral segments of this nucleus. The predominance of positive cells in the caudal area may explain why one previous investigation failed to record responses in rostral caudalis-interpolaris neurons during and after CSD (ref. 21). Because c-fos expression was abolished after chronic trigeminal nerve sectioning or by treatment with a prejunctional 5-HT_{1B/D} receptor agonist sumatriptan²², the evidence suggests that CSD activates meningeal axons and central trigeminal projections associated with nociception.

Discussion

We used a novel method, laser speckle-contrast imaging¹⁶ to acquire simultaneous two-dimensional blood-flow maps of cortical tissue and pial and dural blood vessels. Using this technique,

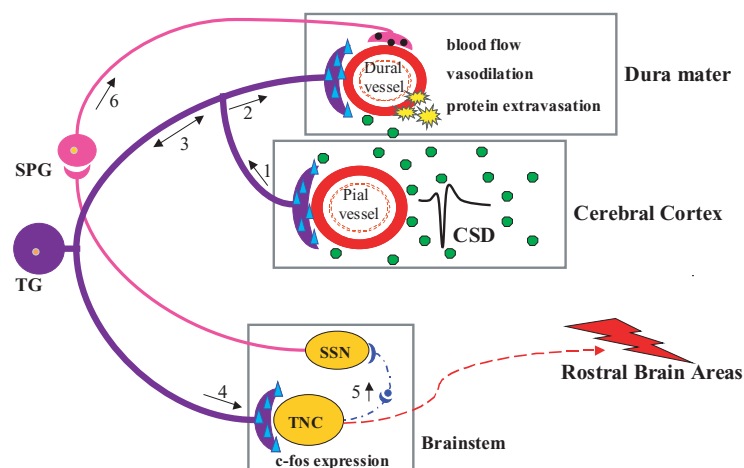


Fig. 4 Proposed mechanism suggesting a link between CSD and trigeminovascular activation. Intense neurometabolic cortical activity such as CSD (illustrated by DC shift in cortex) releases potassium and hydrogen ions, neurotransmitters and metabolites (for example, nitric oxide, adenosine, arachidonate; green circles) into the extracellular and perivascular space and causes transient hyperemia and vasodilation in cortex, pial vessels and dura mater. Within the perivascular space, these molecules activate or sensitize perivascular trigeminal afferents (arrow 1) and transmit impulses centrally to trigeminal ganglia (TG) and trigeminal nucleus caudalis (TNC) (arrows 3 and 4). Impulses from TNC are carried rostrally to brain structures involved in transmitting and processing pain. Dural trigeminal afferents are either directly activated or stimulated indirectly (via bifurcating axons; arrow 2) and possibly sensitized by edema (yellow stars) following the release of vasoactive neuropeptides (substance P, calcitonin gene related peptide, neurokinin A; blue triangles). Activation of ipsilateral TNC in turn, leads to stimulation of the superior salivatory nucleus (SSN; arrow 5) and parasympathetic efferents via the sphenopalatine ganglia (arrow 6). Postganglionic parasympathetics promote vasodilation and augment flow by releasing vasoactive intestinal polypeptide, nitric oxide or acetylcholine (black circles) into the dura mater. As evidence for this central trigeminal-parasympathetic 'reflex', lesioning trigeminal nerve significantly suppressed prolonged blood-flow elevation in the MMA (P2), edema and c-fos expression after CSD. The MMA response was dependent upon trigeminal brainstem inputs based on results after trigeminal rhizotomy. The data are consistent with the formulation that events within brain stimulate trigeminovascular afferents to generate headache and promote MMA vasodilation in an animal model of aura-induced migraine. Note: parasympathetic projections from the sphenopalatine ganglia (SPG) to the pia arachnoidal meninges^{23,45} are not drawn in this figure.

we studied the neurogenic control of MMA blood flow to determine whether CSD—the putative event associated with the development of migraine visual aura—stimulates the trigeminovascular system. CSD augmented MMA blood flow on the affected side by neurogenic mechanisms requiring both trigeminal and parasympathetic innervation. Trigeminal activation (as reflected by MMA flow increase, that is, P2) was observed at around five minutes or after CSD spread across the entire cortex, perhaps reflecting the human condition in which the onset of headaches most typically begins following but not during the migraine aura. CSD also caused unilateral plasma protein leakage within the overlying dura mater and brain-stem activation, both blocked by trigeminal denervation. The evidence supports the formulation that intrinsic neurophysiological cortical events such as CSD irritate axon collateral nociceptors in pia and dura mater (Fig. 4). By so doing, a critical link was established between the experimental basis for migraine visual aura and the genesis of unilateral head pain, an explanation that may also clarify the origins of human headache in other neurological conditions.

Table 1 C-fos-positive cells in trigeminal nucleus caudalis (lamina I, II) following repetitive unilateral CSD

Brainstem below Obex (mm)	Sham ($n=9$)		NCNT ($n=6$)		Sumatriptan ($n=4$)	
	R	L	R	L	R	L
0—1.0	21 ± 1	17 ± 2	17 ± 1	18 ± 1	15 ± 2	13 ± 1
1.0—3.0	89 ± 3*	48 ± 4	49 ± 4	42 ± 4	58 ± 4	50 ± 3
3.0—6.0	81 ± 4	62 ± 4	54 ± 3	52 ± 2	70 ± 6	67 ± 5

*, $P < 0.01$, difference from contralateral side or CSD side after nasociliary nerve transection (NCNT) or sumatriptan treatment. R (right), CSD side; L (left), control side. Data are mean ± s.e.m. of c-fos positive cells per section (50 μ m).

One important finding relates to a long lasting blood-flow rise in a major artery supplying blood to the dura mater, the MMA, which depends on an intact trigeminal and parasympathetic innervation (Figs. 1 and 2). Although little is known about blood-flow regulation within the MMA, increases in flow develop in brain or large pial vessels following electrical trigeminal or parasympathetic stimulation^{23,24}. For example, trigeminal ganglion stimulation enhances carotid artery blood flow via parasympathetic vasodilator fibers from the cat sphenopalatine ganglia²⁵. Trigeminal rhizotomy blocks the carotid artery blood-flow rise after trigeminal stimulation²⁵. Similarly, trigeminal rhizotomy abrogated the MMA response following CSD (Fig. 2b). These results establish with certainty that flow and dilation were dependent upon trigeminal inputs to brainstem (Fig. 4). Furthermore, reflex-like parasympathetic vasodilation accompanies noxious stimulation of other cephalic tissues²⁶. In humans, activation of such pathways explains facial flushing during trigeminal ganglion stimulation²⁷ or reflex activation of parasympathetic pathways in certain headaches leading to tearing and dilation of conjunctival vessels²⁸. Although direct neuronal projections may exist between trigeminal nucleus caudalis and superior salivatory nucleus, they have been difficult to demonstrate. More likely, the flow change may involve polysynaptic connections between the two¹⁷, perhaps after forming synapses within the lateral parabrachial nucleus^{29–31}. Taken together, our data suggest that CSD is a noxious event within cerebral cortex sufficient to activate trigeminal afferents, trigger headache and reflex middle meningeal vasodilation.

We found that sensory-effector mechanisms promoted the extravasation of plasma proteins in the overlying dura mater after a single CSD (Fig. 2). Pretreatment with L-733,060, a selective NK1-receptor antagonist, or trigeminal transection suppressed this response, whereas parasympathetic transection did not. Thus the blood-flow response and edema formation were generated by distinct neuronal mechanisms. The effect of L-733,060 suggests that substance P was released through axon reflex mechanisms from trigeminal fibers³², perhaps after axon collateral nerve endings were stimulated in pia mater during CSD. Upon release from perivascular axons, neuropeptides enhance plasma leakage as documented in many tissues including dura mater²²; mast cells participate as well as endothelial cells. Not surprisingly, proteins did not leak from pial vessels during CSD nor following antidromic trigeminal stimulation because pial blood vessels possess relatively tight endothelial junctions that impede plasma protein leakage¹⁹. In preliminary studies, plasma protein leakage was recently reported in human meninges during migraine and other headaches³³ suggesting similarities between mechanisms.

Several mechanisms may have contributed to peripheral and central trigeminal activation after CSD; these include transient vasodilation, changes in the composition of the extracellular space and protein extravasation in dura mater. Their respective contributions are difficult to dissect with certainty (Fig. 4). Of relevance to blood vessels, Cumberbatch *et al.* found that five minutes of pronounced dural vasodilation after administering CGRP, a potent vasodilator, evoked hyperexcitable responses to innocuous facial stimulation, thereby demonstrating sensitization within central trigeminal neurons³⁴. Although not measured, a sustained high firing rate in central trigeminal neurons could explain the prolonged P2 blood-flow response that lasted as long as 45 minutes after CSD. Vasodilation dur-

ing P1 and P2, however, was more modest than after CGRP infusion³⁴, thereby questioning whether vasodilation by itself was sufficient to cause trigeminal sensitization and activation after CSD. As a second possibility, release of ions and neurotransmitters from neurons and glia that are characteristic of CSD—for example, potassium ions³⁵, protons, arachidonic acid³⁶, nitric oxide and adenosine—depolarized trigeminal axons and dilated meningeal blood vessels. To illustrate, topically applied potassium, protons and prostaglandins discharge and sensitize unmyelinated C fibers in dura mater³⁷; protons and PGE₂ sensitize peripheral afferents by phosphorylation-dependent mechanisms³⁸. All three relax vascular smooth muscle³⁹. Ions and other molecules access the pial surface by gap junctions between astrocyte-pia-arachnoidal cells⁴⁰, whereas venous channels drain cerebral cortex into the dural sinuses. After CSD, epicortical potassium levels rise to 15 mM (ref. 41), which is sufficient to relax vascular smooth muscle and depolarize axonal membranes of primary afferent neurons. Hence, a sequence of events may take place that augments blood flow in MMA (as a possible P1 mechanism), releases vasoactive neuropeptides locally to promote plasma protein leakage and promotes central neurotransmission and reflex parasympathetic activation (Fig. 4). Additionally, peripheral and central trigeminal sensitization may intensify and sustain the pain and augment blood flow.

Although there are no studies measuring the caliber or flow in dural vessels during migraine headache, sensitization does develop as part of an attack⁴². For example, migraineurs describe unpleasant cutaneous sensations in response to non-noxious stimuli (allodynia)⁴² and headaches intensify by events that normally do not cause pain, but raise intracranial pressure and distend venous channels (such as coughing and bending). Vasodilation, long hypothesized to explain the headache of migraine⁴³, developed during CSD as well as after it. The second or more prolonged dilation and hyperemia was initiated and sustained by trigeminal-dependent parasympathetic activation. Thus, vasodilation and flow changes, as first postulated in migraine research by Graham and Wolff⁴³, are fundamental to the pathophysiological events that follow CSD in rodent meninges. However, here we found that sustained vasodilation and augmented flow (P2) did not trigger trigeminal activation and nociception after CSD, but rather developed primarily as a consequence of trigeminal activation (Fig. 2). Hence, the association between dilation and pain may be readily confused in migraine⁴⁴.

Despite differences between rodent and human cortex in complexity of scale, biology of CSD, and cortical development and folding, our data strongly indicate a link between cortical events such as CSD and trigeminovascular activation during migraine with aura. Our findings suggest that the brain generates headache in this subtype in an animal model of migraine. In a related way, auras with motor or sensory symptoms may also represent CSD-like events within primary motor or sensory cortex and could generate migraine headaches by similar mechanisms. Unlike those with aura, the pathophysiology of migraine subtypes without aura is unknown and largely unexplored. We suggest that central nervous system dysfunction is an important provocation, and if so, this would help to understand the associations of migraine with stress, sleep, exercise and epilepsy, among other factors. In other headache disorders, there may be a neurophysiological or metabolic substrate that is not as distinctive as CSD or as easily detected with pre-

sent-day technology, and a blood-flow phenotype has not yet been identified. Nevertheless, our findings indicate that intense perturbations that generate the cellular, molecular and vascular changes in brain akin to CSD can cause the headaches of aura-induced migraine, especially when it develops in proximity to the trigeminovascular innervation in genetically susceptible individuals.

Methods

Animals and experimental setup. Animal protocols were approved by the MGH Subcommittee on Research Animal Care. Male Sprague-Dawley rats ($n = 105$; 250–350 g) were anesthetized intraperitoneally with sodium pentobarbital (60 mg/kg); and rectal temperature, arterial blood pressure, heart rate, arterial blood pH, pO_2 and pCO_2 were monitored. In a stereotaxic frame, frontal (1–3 mm anterior and 2–4 mm lateral to bregma) and occipital craniotomies (7–8 mm posterior and 1–2 mm lateral to bregma) were placed symmetrically over both hemispheres unless otherwise noted. The dura mater was opened 1 h before CSD induction. For imaging MMA blood flow, a craniotomy (2–6 mm posterior and 3–7 mm lateral to bregma) was carefully drilled above the MMA. NCN or postganglionic parasympathetic efferents were transected⁴⁵ or exposed but left intact in sham animals. Trigeminal rhizotomy was performed via a ventromedian skull base craniotomy. Drugs were given as follows: MK-801 (5 mM, topically applied to cortex in the anterior craniotomy site (7–9 mm remote from MMA) 15 min before CSD), sumatriptan (300 μ g/kg, i.v., 15 min pretreatment), and L-733,066 (1mg/kg, i.v., 1 h pretreatment).

CSD protocol. Cortical steady potential (DC) and electrocorticogram were recorded by single barreled-glass microelectrodes inserted 900 μ m into cortex or placed on the surface to prevent CSD during electrode insertion. To avoid triggering meningeal afferents, CSD was induced either by pinprick (30 G needle) or by bipolar parallel electrode (0.5-mm tip exposed) inserted 1 mm into cortex (1 mA, 300 ms pulse). Electrical stimulation or pinprick was evoked 1.5 mm anterior to the recording electrode or 9 mm from a recording electrode in the occipital region. When CSD was induced by either pinprick or electrical stimulation, the electrophysiological responses did not differ between paradigms ($n = 12$). Hence, one or both methods were used for CSD induction. As specified, one or more CSDs were used for blood-flow and edema experiments. For c-fos expression, multiple CSDs ($n = 7$) were evoked^{21,31} to increase signal-to-noise ratio.

Laser speckle-contrast imaging of blood flow. A laser diode (780 nm) and CCD camera were positioned above the craniotomy such that a 1.75 \times 2.5 mm area was imaged. Blood flow was imaged 2 min before CSD induction and continued for 1 h. Ten raw speckle images were acquired at 15 Hz at 5-s intervals for 60 min and a speckle-contrast image was computed for each raw speckle image. Speckle contrast is a measure of speckle visibility, which is related to the motion of the scattering particles and therefore blood flow. Each set of 10 speckle-contrast images was averaged together. A relative blood-flow image (percentage of baseline) was then obtained by converting the speckle-contrast values to correlation time values which were assumed to be inversely proportional to flow velocity¹⁶, and dividing by a baseline image obtained before CSD induction.

To compute the MMA relative blood flow, first a threshold was set in a region of interest (ROI) from the baseline speckle-contrast image and the MMA was identified by pixels with speckle-contrast values below this threshold. Once the MMA ROI was identified, the mean values of the relative blood flow in those pixels were computed at each time-point. The time-course of the blood-flow changes in cortex or pial vessels was obtained from the same images in a similar fashion. When vessel diameter was measured, the laser source was replaced with green light illumination (570 \pm 10 nm). Vessel diameter changes were analyzed with image-processing software (Matlab, The Mathworks, Inc., Natick, Massachusetts) and the data expressed as a percentage change in baseline diameter during the same experiment.

Plasma protein extravasation studies. HRP (type VI, Sigma) was infused i.v. over 1 h (60 mg/kg in saline) beginning just before the CSD induction. One, two, four or six CSDs were induced by pinprick or electrically ($n = 13$). For the denervation experiments ($n = 17$), plasma leakage was assessed after CSD induced by electrical stimulation every 15 min for 90 min (total 6). Rats were killed after the last CSD by cardiac perfusion and the dura mater was processed using the diaminobenzidine reaction. Protein leakage (HRP intensity and distribution) was assessed in dura mater within 4 symmetrical fields by 2 trained investigators naive to the protocol and rated by minimal leakage–maximal intensity (0–4). Values were assigned and compared between sides. Data presented as ratio of leakage within dura mater on the CSD side compared with the control side either in normal animals or after denervation. Following L-733,060 treatment, leakage was compared on the CSD side with the contralateral dura mater. Staining intensity was also analyzed by using image analysis software (Matlab).

C-fos studies. Two hours after CSD, rats were perfused with fixative and then processed for c-fos immunohistochemistry as described³¹. Every 150 μ m, sections (50- μ m thick) were taken for immunostaining and cells counted from obex to C3.

Statistical analysis. Data are presented as the mean \pm s.e.m. Blood-flow and c-fos data were analyzed using one-way analysis of variance followed by Bonferroni test. Edema score was analyzed by Mann–Whitney U test. $P < 0.05$ was considered significant.

Acknowledgments

We thank M. Foley for assistance and T. Dalkara for critical review of the manuscript. This study was supported by the NIH Migraine Program Project 2P01 NS10828 (to M.A.M.), NIH 1R29NS38842 (to D.A.B.), NIH K25 NS41291-01 (to A.K.D.), IHS research fellowship and Deutsche Forschungsgemeinschaft Re 1316-1 (to U.R.).

Competing interests statement

The authors declare that they have no competing financial interests.

RECEIVED 30 NOVEMBER; ACCEPTED 18 DECEMBER, 2001

1. Penfield, W. & McNaughton, F. Dural headache and innervation of the dura mater. *Arch. Neurol. Psychiat.* **44**, 43–75 (1940).
2. Ray, B.S. & Wolff, H.G. Experimental studies on headache: pain sensitive structures of the head and their significance in headache. *Arch. Surg.* **41**, 813–856 (1940).
3. Moskowitz, M.A. The visceral organ brain: implications for the pathophysiology of vascular head pain. *Neurology* **41**, 182–186 (1991).
4. Mayberg, M., Langer, R.S., Zervas, N.T. & Moskowitz, M.A. Perivascular meningeal projections from cat trigeminal ganglia: possible pathway for vascular headaches in man. *Science* **213**, 228–230 (1981).
5. O'Connor, T.P. & van der Kooy, D. Pattern of intracranial and extracranial projections of trigeminal ganglion cells. *J. Neurosci.* **6**, 2200–2207 (1986).
6. Liu-Chen, L.Y., Han, D.H. & Moskowitz, M.A. Pia arachnoid contains substance P originating from trigeminal neurons. *Neuroscience* **9**, 803–808 (1983).
7. Edvinsson, L., McCulloch, J. & Uddman, R. Substance P: immunohistochemical localization and effect upon cat pial arteries *in vitro* and *in situ*. *J. Physiol.* **318**, 251–258 (1981).
8. Uddman, R., Hara, H. & Edvinsson, L. Neuronal pathways to the rat middle meningeal artery revealed by retrograde tracing and immunocytochemistry. *J. Auton. Nerv. Syst.* **26**, 69–75 (1989).
9. Suzuki, N., Hardebo, J.E. & Owman, C. Origins and pathways of cerebrovascular nerves storing substance P and calcitonin gene-related peptide in rat. *Neuroscience* **31**, 427–438 (1989).
10. Feindel, W., Penfield, W. & McNaughton, F. The tentorial nerves and localization of intracranial pain in man. *Neurology* **10**, 555–563 (1960).
11. Hadjikhani, N. *et al.* Mechanisms of migraine aura revealed by functional MRI in human visual cortex. *Proc. Natl. Acad. Sci. USA* **98**, 4687–4692 (2001).
12. Cao, Y., Welch, K.M., Aurora, S. & Vikingstad, E.M. Functional MRI-BOLD of visually triggered headache in patients with migraine. *Arch. Neurol.* **56**, 548–554 (1999).
13. Lauritzen, M. & Olesen, J. Regional cerebral blood flow during migraine attacks by Xenon-133 inhalation and emission tomography. *Brain* **107**, 447–461 (1984).
14. Leao, A. Spreading depression of activity in the cerebral cortex. *J. Neurophysiol.* **7** (1944).
15. Moskowitz, M.A. The neurobiology of vascular head pain. *Ann. Neurol.* **16**, 157–168 (1984).

16. Dunn, A.K., Bolay, H., Moskowitz, M.A. & Boas, D.A. Dynamic imaging of cerebral blood flow using laser speckle. *J. Cereb. Blood Flow Metab.* **21**, 195–201 (2001).
17. Goadsby, P.J. & Duckworth, J.W. Effect of stimulation of trigeminal ganglion on regional cerebral blood flow in cats. *Am. J. Physiol.* **253**, R270–274 (1987).
18. Williamson, D.J., Hargreaves, R.J., Hill, R.G. & Shephard, S.L. Intravital microscope studies on the effect of neurokinin agonists and calcitonin gene-related peptide on dural vessel diameter in anaesthetized rat. *Cephalalgia* **17**, 518–524 (1997).
19. Markowitz, S., Saito, K. & Moskowitz, M.A. Neurogenically mediated leakage of plasma protein occurs from blood vessels in dura mater but not brain. *J. Neurosci.* **7**, 4129–4136 (1987).
20. Hunt, S.P., Pini, A. & Evan, G. Induction of c-fos-like protein in spinal cord neurons following sensory stimulation. *Nature* **328**, 632–634 (1987).
21. Ebersberger, A., Schaible, H.G., Averbeck, B. & Richter, F. Is there a correlation between spreading depression, neurogenic inflammation, and nociception that might cause migraine headache? *Ann. Neurol.* **49**, 7–13 (2001).
22. Buzzi, M.G. & Moskowitz, M.A. The antimigraine drug, sumatriptan (GR43175), selectively blocks neurogenic plasma extravasation from blood vessels in dura mater. *Br. J. Pharmacol.* **99**, 202–206 (1990).
23. Suzuki, N., Hardebo, J.E., Kahrstrom, J. & Owman, C. Selective electrical stimulation of postganglionic cerebrovascular parasympathetic nerve fibers originating from the sphenopalatine ganglion enhances cortical blood flow in the rat. *J. Cereb. Blood Flow Metab.* **10**, 383–391 (1990).
24. Suzuki, N., Hardebo, J.E., Kahrstrom, J. & Owman, C. Effect on cortical blood flow of electrical stimulation of trigeminal cerebrovascular nerve fibres in the rat. *Acta Physiol. Scand.* **138**, 307–316 (1990).
25. Lambert, G.A., Bogduk, N., Goadsby, P.J., Duckworth, J.W. & Lance, J.W. Decreased carotid arterial resistance in cats in response to trigeminal stimulation. *J. Neurosurg.* **61**, 307–315 (1984).
26. Drummond, P.D. The effect of sympathetic blockade on facial sweating and cutaneous vascular responses to painful stimulation of the eye. *Brain* **116**, 233–241 (1993).
27. Drummond, P.D., Gonski, A. & Lance, J.W. Facial flushing after thermocoagulation of the Gasserian ganglion. *J. Neurol. Neurosurg. Psychiatry* **46**, 611–616 (1983).
28. Moskowitz, M.A. Cluster headache: evidence for a pathophysiologic focus in the superior pericarotid cavernous sinus plexus. *Headache* **28**, 584–586 (1988).
29. Spencer, S.E., Sawyer, W.B., Wada, H., Platt, K.B. & Loewy, A.D. CNS projections to the pterygopalatine parasympathetic preganglionic neurons in the rat: a retrograde transneuronal viral cell body labeling study. *Brain Res.* **534**, 149–169 (1990).
30. Allen, G.V., Barbrick, B. & Esser, M.J. Trigeminal-parabrachial connections: possible pathway for nociception-induced cardiovascular reflex responses. *Brain Res.* **715**, 125–135 (1996).
31. Moskowitz, M.A., Nozaki, K. & Kraig, R.P. Neocortical spreading depression provokes the expression of c-fos protein-like immunoreactivity within trigeminal nucleus caudalis via trigeminovascular mechanisms. *J. Neurosci.* **13**, 1167–1177 (1993).
32. Lee, W.S., Moussaoui, S.M. & Moskowitz, M.A. Blockade by oral or parenteral RPR 100893 (a non-peptide NK1 receptor antagonist) of neurogenic plasma protein extravasation within guinea-pig dura mater and conjunctiva. *Br. J. Pharmacol.* **112**, 920–924 (1994).
33. Göbel, N. *et al.* Evidence of regional plasma protein extravasation in cluster headache using Tc-99m albumin SPECT. *Cephalalgia* **20**, 287 (2000).
34. Cumberbatch, M.J., Williamson, D.J., Mason, G.S., Hill, R.G. & Hargreaves, R.J. Dural vasodilation causes a sensitization of rat caudal trigeminal neurones in vivo that is blocked by a 5-HT_{1B/1D} agonist. *Br. J. Pharmacol.* **126**, 1478–1486 (1999).
35. Kraig, R.P. & Nicholson, C. Extracellular ionic variations during spreading depression. *Neuroscience* **3**, 1045–1059 (1978).
36. Lauritzen, M., Hansen, A.J., Kronborg, D. & Wieloch, T. Cortical spreading depression is associated with arachidonic acid accumulation and preservation of energy charge. *J. Cereb. Blood Flow Metab.* **10**, 115–122 (1990).
37. Strassman, A.M., Raymond, S.A. & Burstein, R. Sensitization of meningeal sensory neurons and the origin of headaches. *Nature* **384**, 560–564 (1996).
38. Woolf, C.J. & Salter, M.W. Neuronal plasticity: increasing the gain in pain. *Science* **288**, 1765–1768 (2000).
39. Kuschinsky, W. & Wahl, M. Local chemical and neurogenic regulation of cerebral vascular resistance. *Physiol. Rev.* **58**, 656–689 (1978).
40. Grafstein, B., Liu, S., Cotrina, M.L., Goldman, S.A. & Nedergaard, M. Meningeal cells can communicate with astrocytes by calcium signaling. *Ann. Neurol.* **47**, 18–25 (2000).
41. Richter, F. & Schaible, H.G. Spreading depression related DC potential and potassium concentration changes recorded at dura mater in rats. *Eur. J. Neurosci.* **10**, 135 (1998).
42. Burstein, R., Yarnitsky, D., Goor-Aryeh, I., Ransil, B.J. & Bajwa, Z.H. An association between migraine and cutaneous allodynia. *Ann. Neurol.* **47**, 614–624 (2000).
43. Graham, J.R. & Wolff, H.G. Mechanism of migraine headache and action of ergotamine tartrate. *Arch. Neurol. Psychiat.* **39**, 737–763 (1938).
44. Ferrari, M.D. & Saxena, P.R. Clinical and experimental effects of sumatriptan in humans. *Trends Pharmacol. Sci.* **14**, 129–133 (1993).
45. Suzuki, N., Hardebo, J.E. & Owman, C. Origins and pathways of cerebrovascular vasoactive intestinal polypeptide-positive nerves in rat. *J. Cereb. Blood Flow Metab.* **8**, 697–712 (1988).